Bulletin of the Earthquake
Research Institute
Vol. 47 (1969), pp. 165-184

11. A Long Wave around a Breakwater [VI]. —Case of Lateral Incidence—

By Takao Momoi,

Earthquake Research Institute.

(Read Jan. 28, 1969.—Received Jan. 30, 1969.)

Abstract

The long wave around the breakwater for the case of lateral incidence of the invading wave (along the breakwater) is discussed through the numerical calculation. The calculated waves are the RST (resultant) wave, the reflected wave from the leeward breakwater for the model of the double breakwater wings, and the RST wave for the model of the single breakwater wing, the last of which is based on Stoker's theory (*Stoker*, 1965). The most conspicuous feature is an appearance of the reflected (emitting) wave from the nearby part of the terminus of the leeward breakwater for the model of the twin breakwaters.

1. Introduction

Succeeding the previous works (*Momoi*, 1967a, 1967b, 1968a, 1968b and 1968c) concerning the long wave around the breakwater gap, we have discussed, in this report, the long wave around the breakwater for the case of lateral incidence of a train of periodic waves (refer to Fig. 1).

2. RST Wave

In this section, the further numerical calculations of the RST (which is the abbreviation of resultant) wave is made in the range $kd=$ 4.0 to 10.0 (k: the wave number of the incident wave and d: the half width of the breakwater gap) following the procedure mentioned in Section 2,7 of the fourth report (*Momoi*, 1968b). The calculated result are shown in Figs. 2*aw* (*pw*, *al*, *pl*) to 8*aw* (*pw*, *al*,

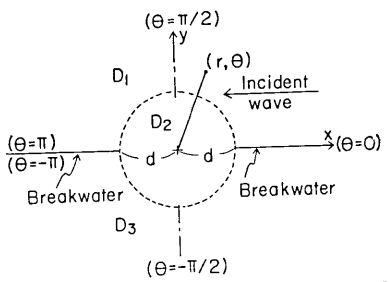

Fig. 1. Geometry of the model used.

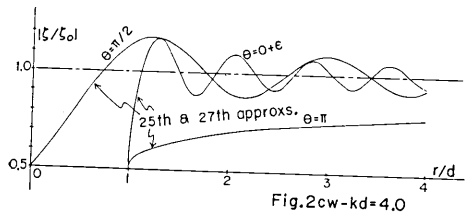

Fig.2cw-kd=4.0

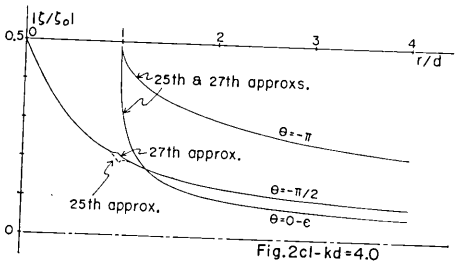

Fig.2cl-kd=4.0

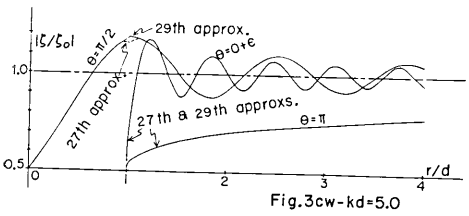

Fig.3cw-kd=5.0

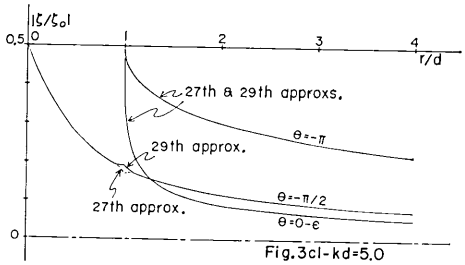

Fig.3cl-kd=5.0

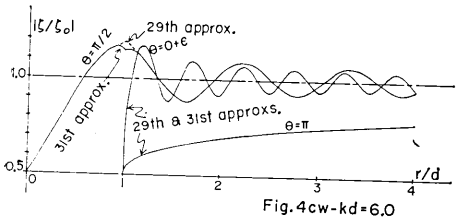

Fig.4cw-kd=6.0

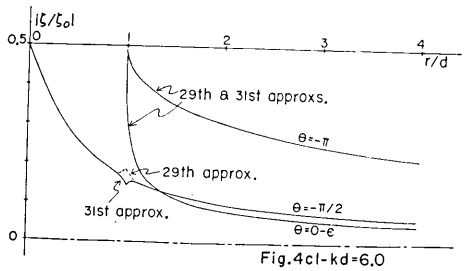

Fig.4cl-kd=6.0

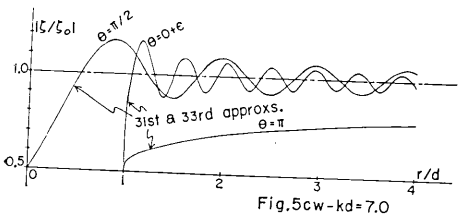

Fig.5cw-kd=7.0

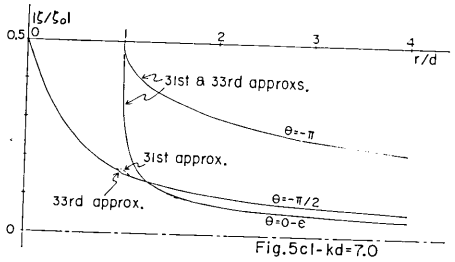

Fig.5cl-kd=7.0

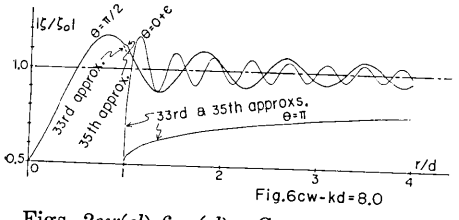

Fig.6cw-kd=8.0

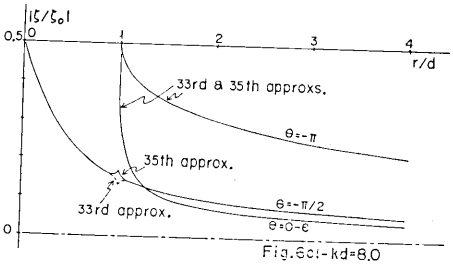

Fig.6cl-kd=8.0

Figs. 2*cw*(*cl*)-6*cw*(*cl*). Convergence check of the approximated theory in the windward (leeward) waters for $kd=4.0\sim8.0$. The subscript *cw* and *cl* denote the figures relevant to the windward and leeward waters.

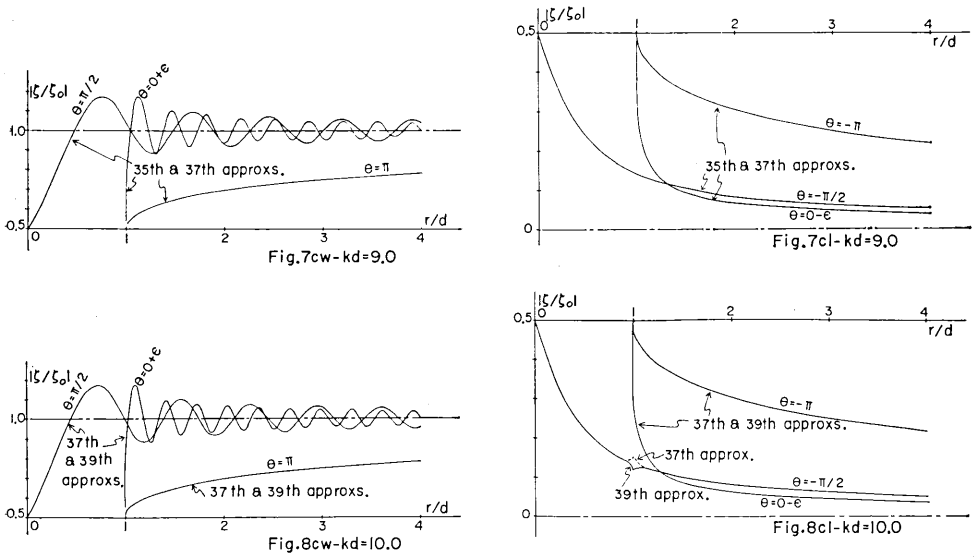

Figs. 7*cw*(*cl*)-8*cw*(*cl*). Convergence check of the approximated theory in the windward (leeward) waters for $kd=9.0\sim10.0$. The subscript *cw* and *cl* denote the figures relevant to the windward and leeward waters.

pl).* The stated values in the figures relevant to the amplitude and phase denote, respectively, $|\zeta/\zeta_0|$ and arg ζ (ζ: the wave height and ζ_0: that of the incident wave). The convergence check of the employed approximation is made in Figs. 2*cw* (*cl*) to 8*cw* (*cl*) through the calculation of the wave height in the directions of $\theta=0\pm\varepsilon$, $\pm\pi/2$ and $\pm\pi\mp\varepsilon$ (ε: the positive infinitesimal and, for the definition of the coordinate θ, the reader should refer to Fig. 1). According to these figures, the convergence of the approximation used is very good except the region near $r/d=1.0$ (r: the azimuthal component of the polar coordinate (refer to Fig. 1)). In drawing the figures concerning the overall variation, the above region is interpolated appropriately by hand.

Before discussing the overall variations of the amplitude and phase around the breakwater gap, those around the terminus of a single breakwater wing are calculated by use of Stoker's solution (*Stoker*, 1957), *i.e.*,

$$\zeta_{single}=\varepsilon J_0(kr)+2\varepsilon\sum_{n=1}^{\infty}e^{i(n\pi/4)}J_{n/2}(kr)\cos\frac{n\alpha}{2}\cos\frac{n\theta}{2}\,, \qquad (1)$$

* The approximations used in depicting these pictures are, respectively, the 27th approximation for Fig. 2*aw* (*pw*, *al*, *pl*), the 29th approximation for Fig. 3*aw* (*pw*, *al*, *pl*), the 31st approximation for Fig. 4*aw* (*pw*, *al*, *pl*), the 33rd approximation for Fig. 5*aw* (*pw*, *al*, *pl*), the 35th approximation for Fig. 5*aw* (*pw*, *al*, *pl*), the 37th approximation for Fig. 7*aw* (*pw*, *al*, *pl*) and the 39th approximation for Fig. 8*aw* (*pw*, *al*, *pl*).

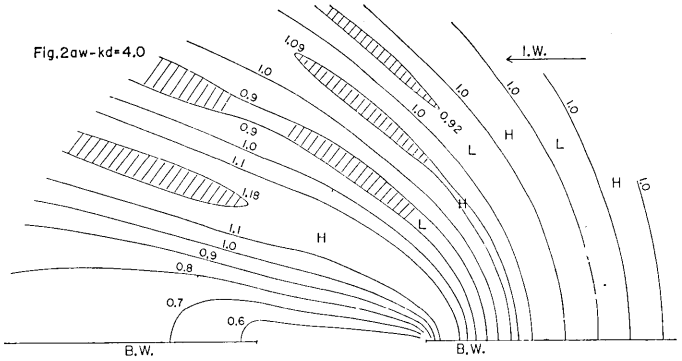

Fig. 2*aw*. Amplitude in the windward waters.

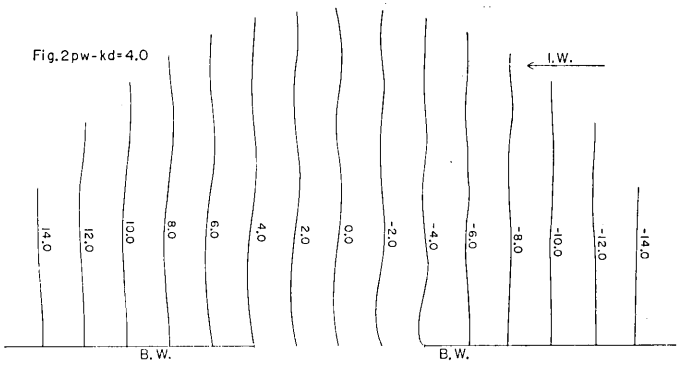

Fig. 2*pw*. Phase in the windward waters.

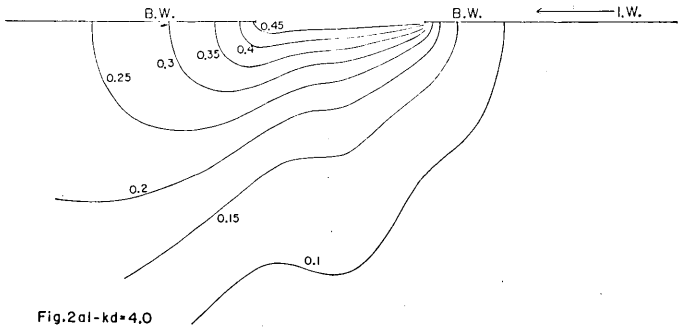

Fig. 2*al*. Amplitude in the leeward waters.

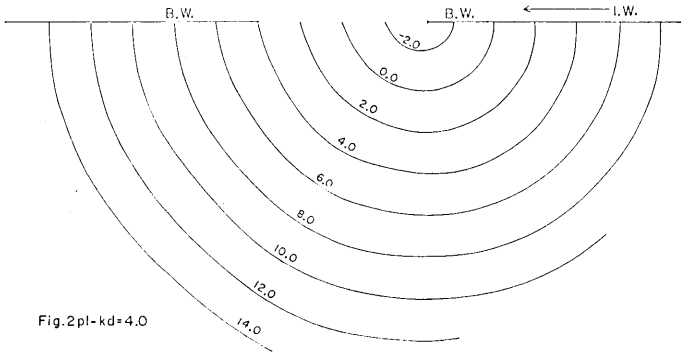

Fig. 2*pl*. Phase in the leeward waters.

Figs. 2*aw*-2*pl*. Variations of the wave around the breakwater gap for kd=4.0.*

* **I. W.** and **B. W.** stated in the figures denote "incident wave" and "breakwater".

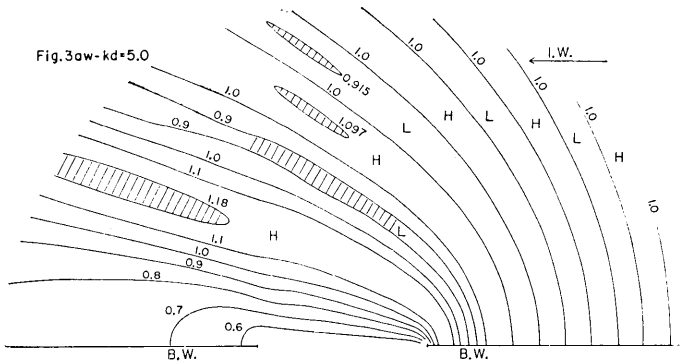

Fig. 3*aw*. Amplitude in the windward waters.

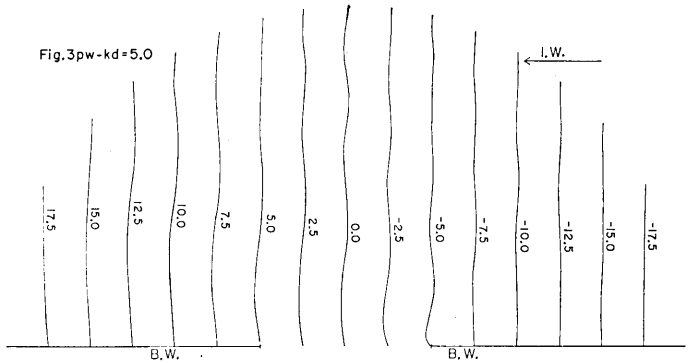

Fig. 3*pw*. Phase in the windward waters.

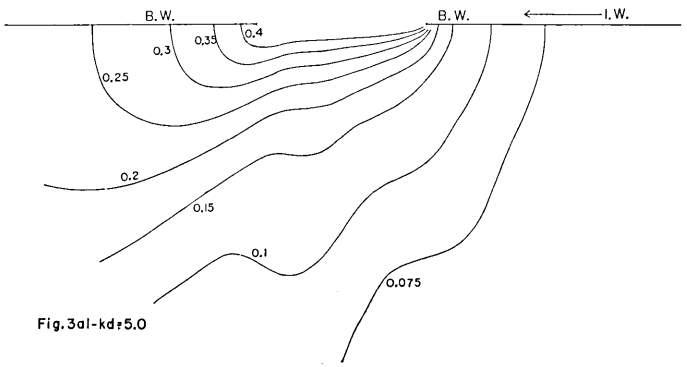

Fig. 3*al*. Amplitude in the leeward waters.

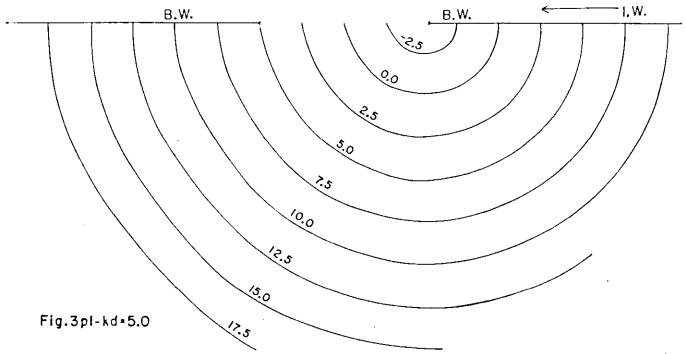

Fig. 3*pl*. Phase in the leeward waters.

Figs. 3*aw*–3*pl*. Variations of the wave around the breakwater gap for $kd=5.0$.*

* See the footnote in Figs. 2*aw*–2*pl*.

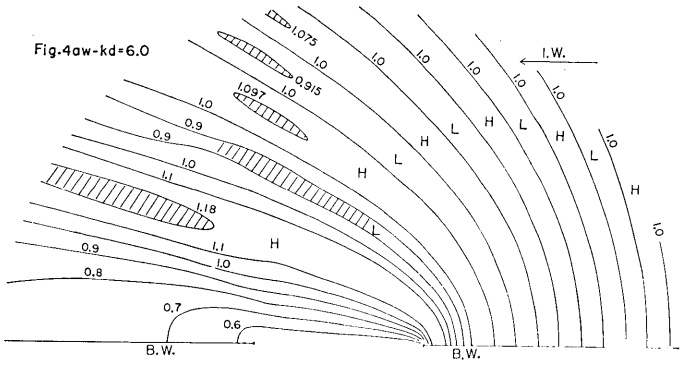

Fig. 4*aw*. Amplitude in the windward waters.

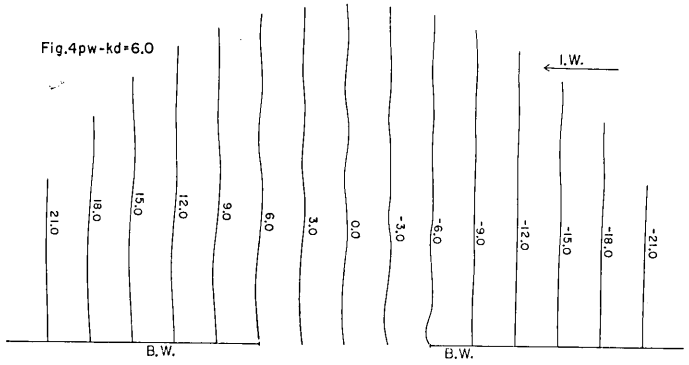

Fig. 4*pw*. Phase in the windward waters.

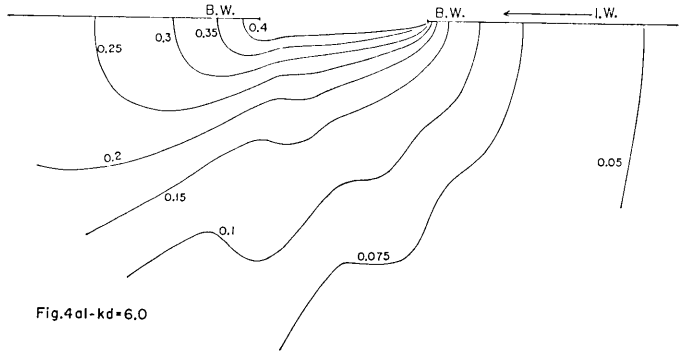

Fig. 4*al*. Amplitude in the leeward waters.

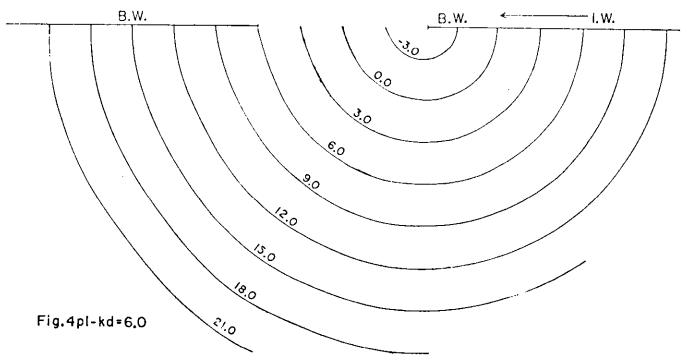

Fig. 4*pl*. Phase in the leeward waters.

Figs. 4*aw*-4*pl*. Variations of the wave around the breakwater gap for kd=6.0.*

* See the footnote in Figs. 2*aw*-2*pl*.

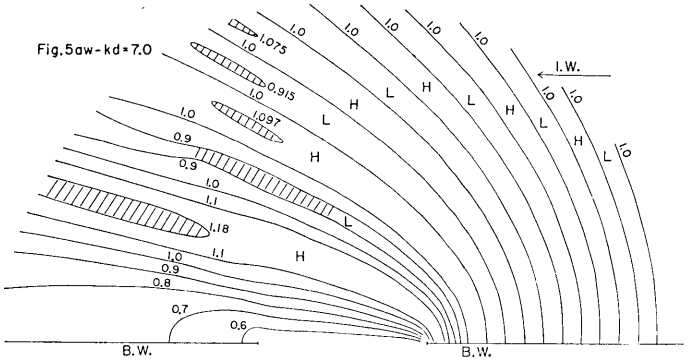

Fig. 5*aw*. Amplitude in the windward waters.

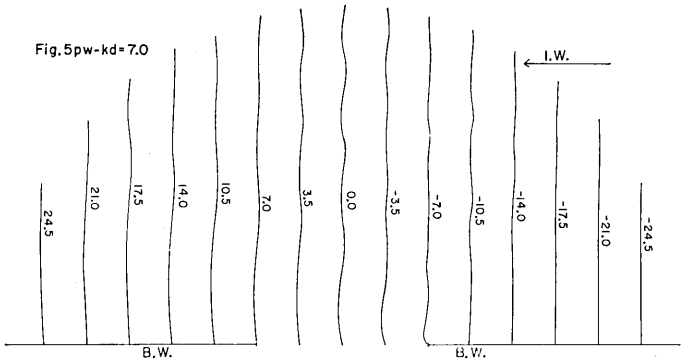

Fig. 5*pw*. Phase in the windward waters.

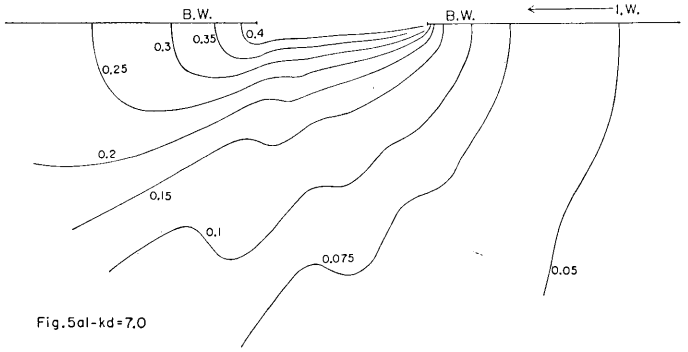

Fig. 5*al*. Amplitude in the leeward waters.

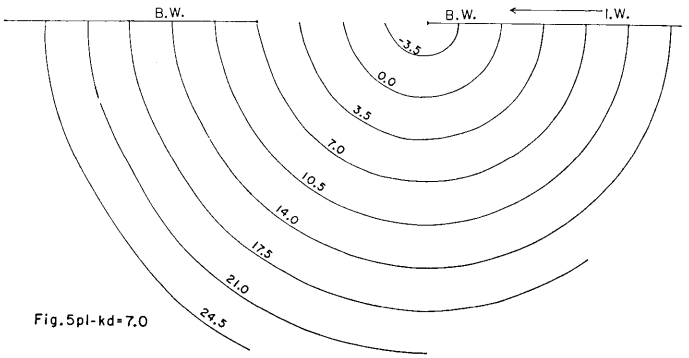

Fig. 5*pl*. Phase in the leeward waters.

Figs. 5*aw*-5*pl*. Variations of the wave around the breakwater gap for kd=7.0.*

* See the footnote in Figs. 2*aw*-2*pl*.

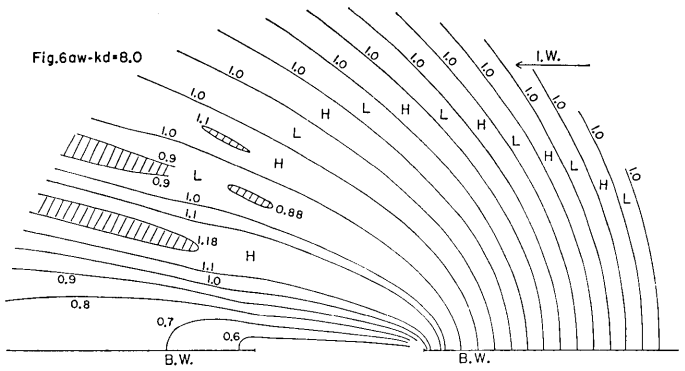

Fig. 6*aw*. Amplitude in the windward waters.

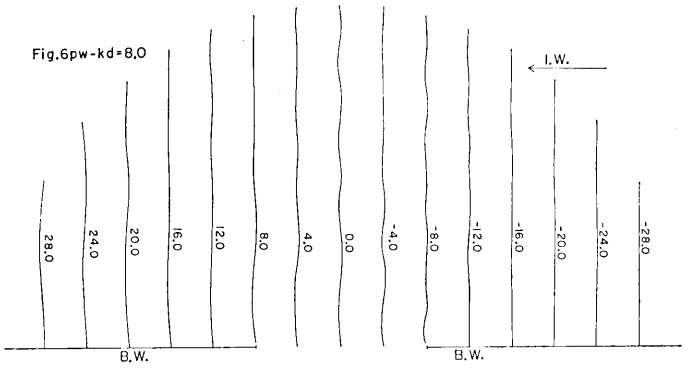

Fig. 6*pw*. Phase in the windward waters.

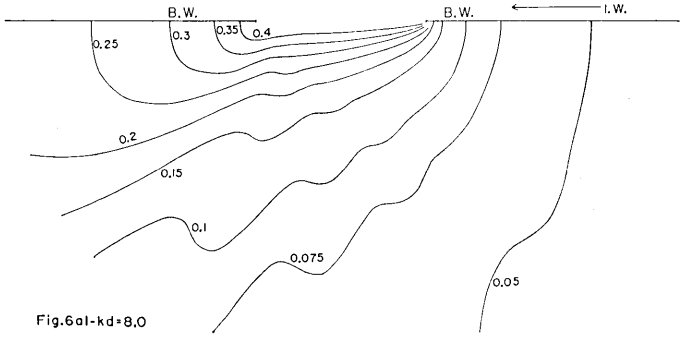

Fig. 6*al*. Amplitude in the leeward waters.

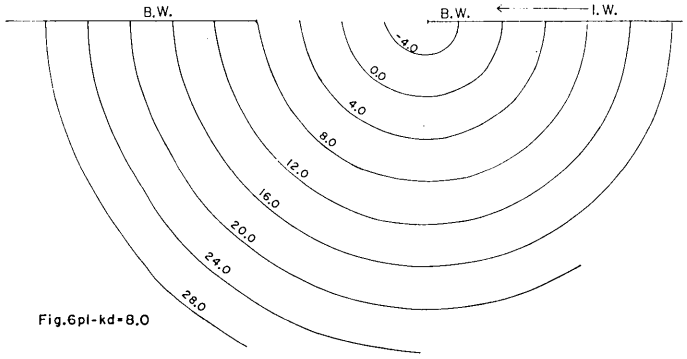

Fig. 6*pl*. Phase in the leeward waters.

Figs. 6*aw*-6*pl*. Variations of the wave around the breakwater gap for kd=8.0.*

* See the footnote in Figs. 2*aw*-2*pl*.

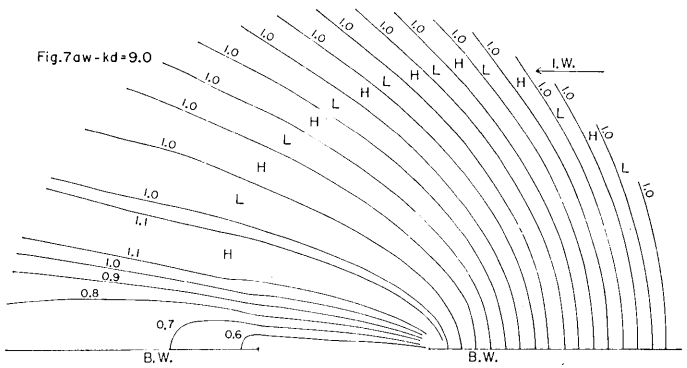

Fig. 7*aw*. Amplitude in the windward waters.

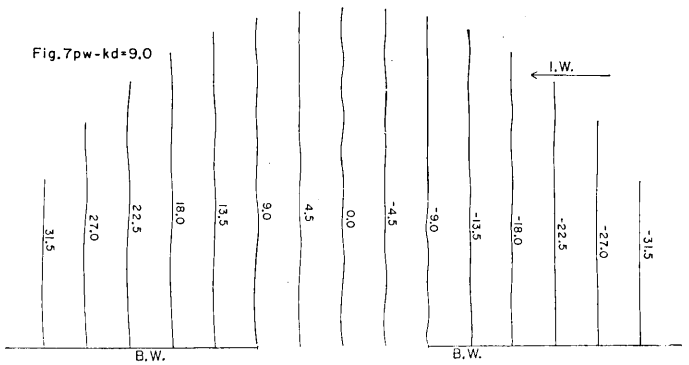

Fig. 7*pw*. Phase in the windward waters.

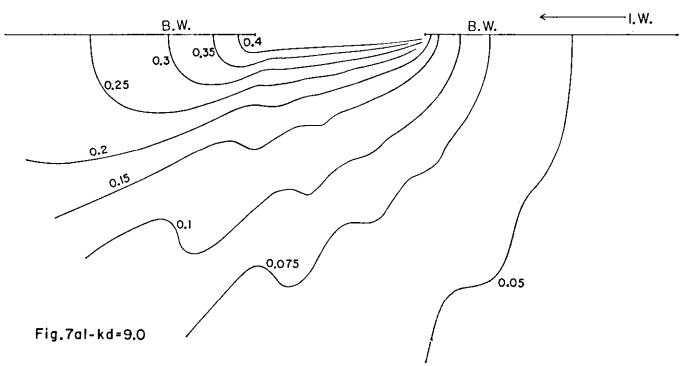

Fig. 7*al*. Amplitude in the leeward waters.

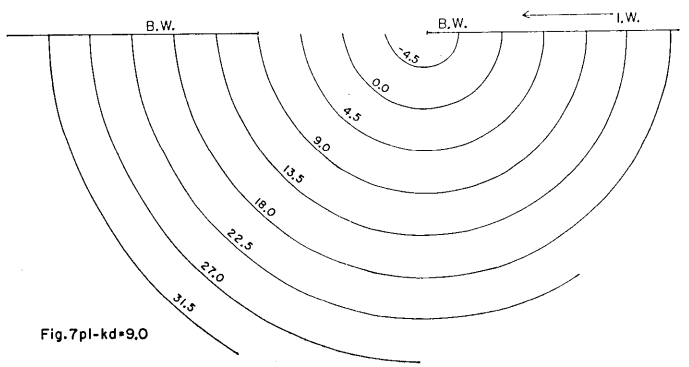

Fig. 7*pl*. Phase in the leeward waters.

Figs. 7*aw*-7*pl*. Variations of the wave around the breakwater gap for $kd=9.0$.*

* See the footnote in Figs. 2*aw*-2*pl*.

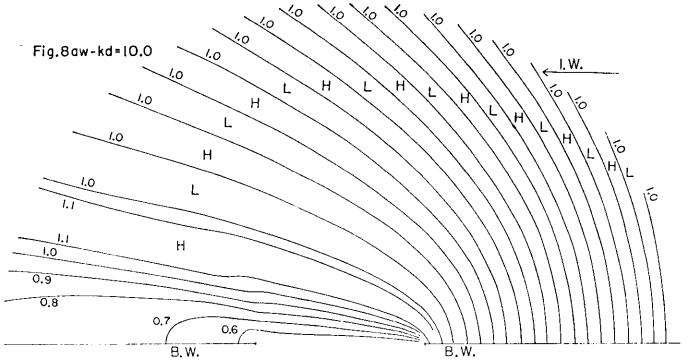

Fig. 8*aw*. Amplitude in the windward waters.

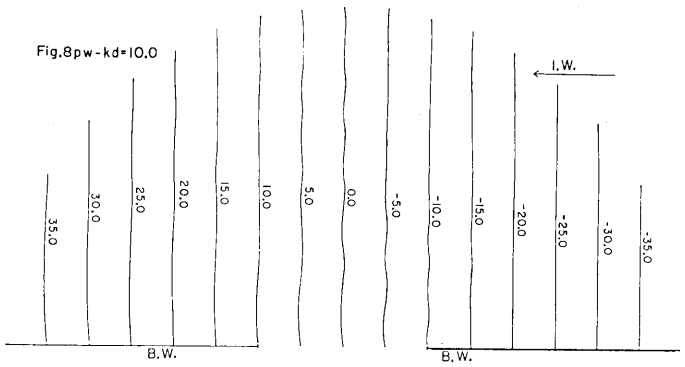

Fig. 8*pw*. Phase in the windward waters.

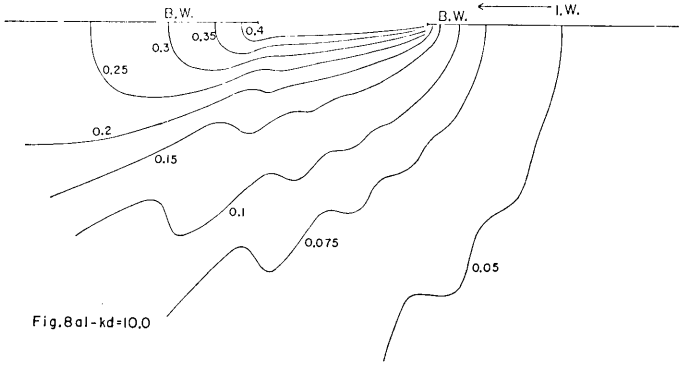

Fig. 8*al*. Amplitude in the leeward waters.

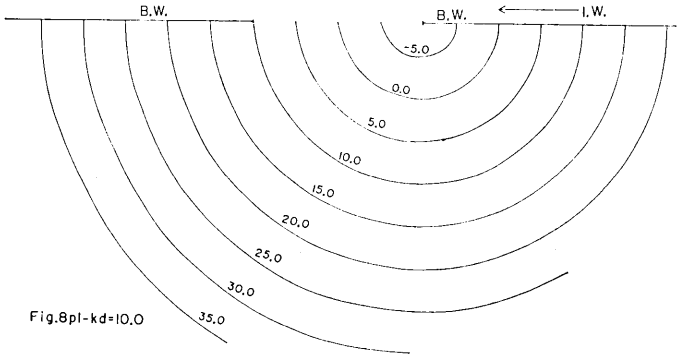

Fig. 8*pl*. Phase in the leeward waters.

Figs. 8*aw*-8*pl*. Variations of the wave around the breakwater gap for $kd=10.0$.*

* See the footnote in Figs. 2*aw*-2*pl*.

where the definition and notation are given in Fig. 9, $\varepsilon=1$ for $\alpha \neq 0$ $\varepsilon=1/2$ for $\alpha=0$, and ζ_{single} is the solution of the equation

$$\left(\frac{\partial^2}{\partial x^2}+\frac{\partial^2}{\partial y^2}+k^2\right)\zeta_{single}=0$$

(in the cartesian coordinate).

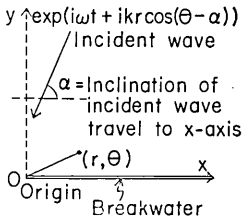

Fig. 9. Nomenclature for the model of the single breakwater wing.

The computed results for $\alpha=0$ are presented in Figs. $10a(p)$ to $14a(p)$ in the range $kr=0$ to 15.0, in which the stated values denote, respectively, $|\zeta_{single}|$ and arg ζ_{single} for the amplitude and phase.

Now, let us proceed with the discussion of the variations of the amplitude and phase around the gap of the double breakwater wings comparing with the case of the single breakwater.

To begin with, the amplitude variation in the windward waters is discussed (refer to Figs. $2aw$ to $8aw$). Comparing Figs. $2aw$ to $8aw$ with Figs. $10a$ to $14a$, the differences of the variations of these two cases are in that (i) the contours extending from the windward breakwater toward the leeward arrive at the leeward breakwater for the case of the double breakwater, while those for the case of the single breakwater run monotonically toward the leeward direction, and (ii) the regions of high and low amplitude appear alternately in the case of the former, while such a behavior is not found in the case of the latter (refer to Fig. 15). The above two phenomena for the case of the double breakwater are as the result of the reflection of the invading waves form the leeward breakwater, which will be further ascertained in the later paper.

Figs. $2pw$ to $8pw$ relevant to the phase variation in the windward waters show that, as kd increases, the component advancing toward the leeward waters through the breakwater gap becomes smaller and smaller.

As far as the variations of the wave in the leeward waters are concerned, the elongation of the contours of the amplitude along the leeward breakwater wing begins to be remarkable with the increase of kd (Figs. $2al$ to $8al$). Comparing Figs. $2al$ to $8al$ with Figs. $10a$ to $14a$, it is found that the contours of the amplitude in the case of the double breakwater have fluctating variation, while those in the single breakwater extend to the leeward side with smooth variation (refer to Fig. 16). The difference is considered to be produced by the wave diffracted from the leeward breakwater. This point will be examined in the later paper.

As for the phase variation in the leeward waters, the following

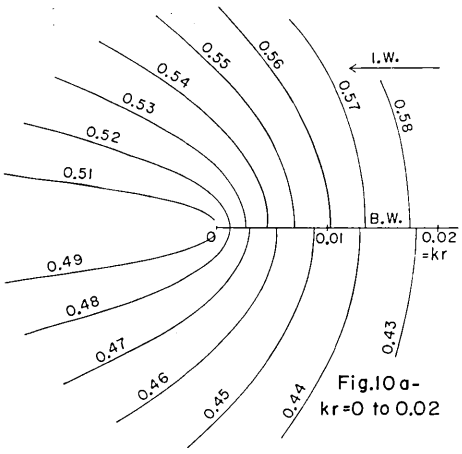

Fig.10a-
kr=0 to 0.02

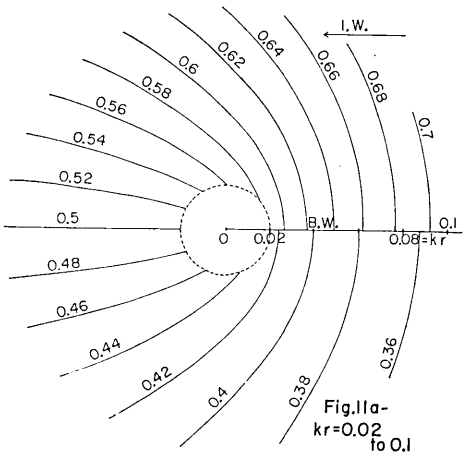

Fig.11a-
kr=0.02 to 0.1

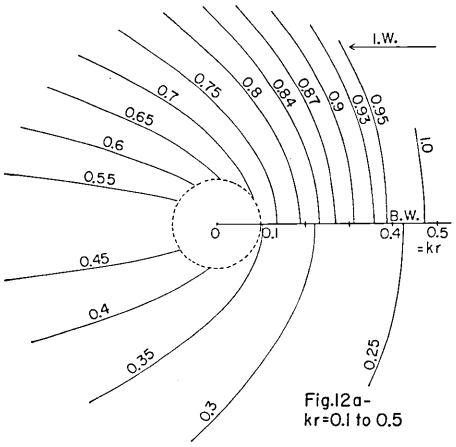

Fig.12a-
kr=0.1 to 0.5

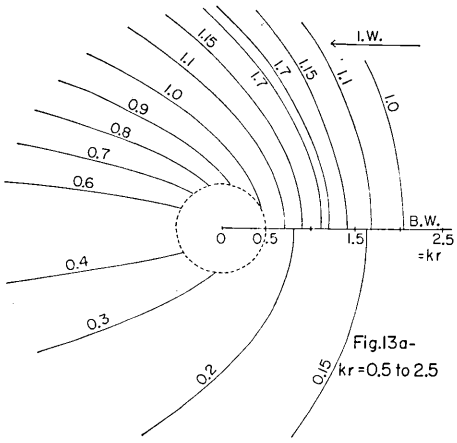

Fig.13a-
kr=0.5 to 2.5

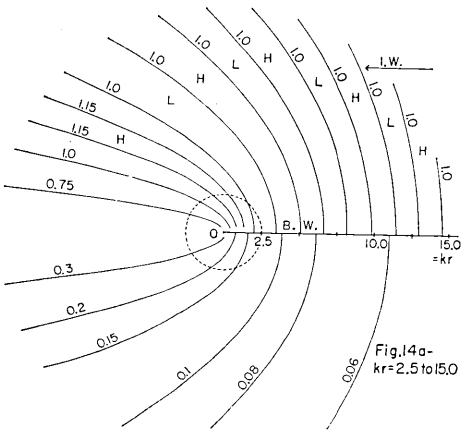

Fig.14a-
kr=2.5 to 15.0

Figs. 10*a*–14*a*. Variation of the amplitude around the terminus of the single breakwater wing for lateral incidence (based on Stoker's theory). **I. W.** and **B. W.** stated in the figures are the abbreviation of "indident wave" and "breakwater".

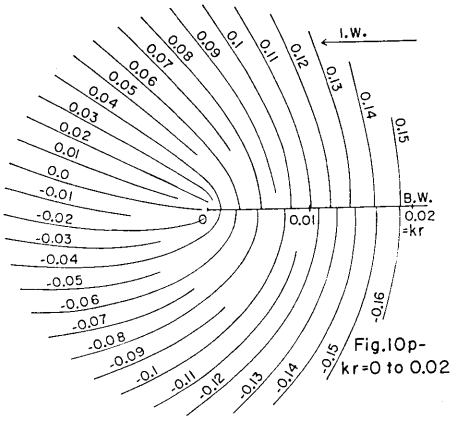

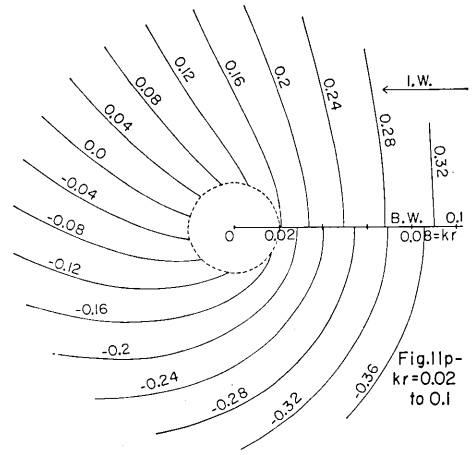

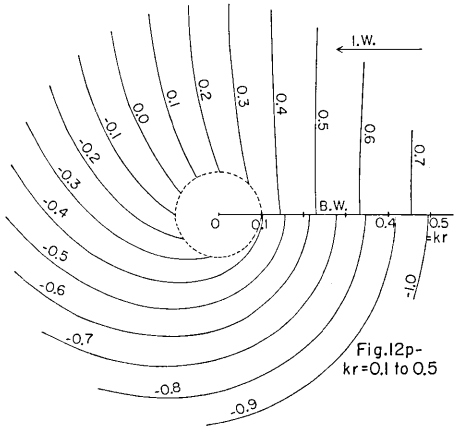

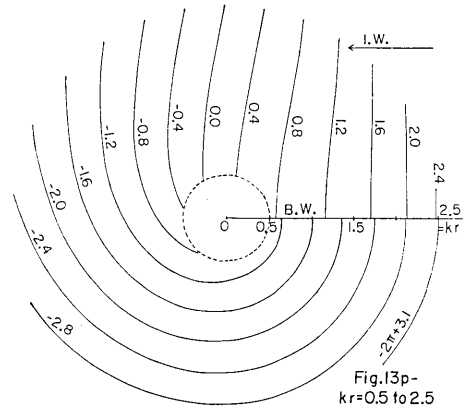

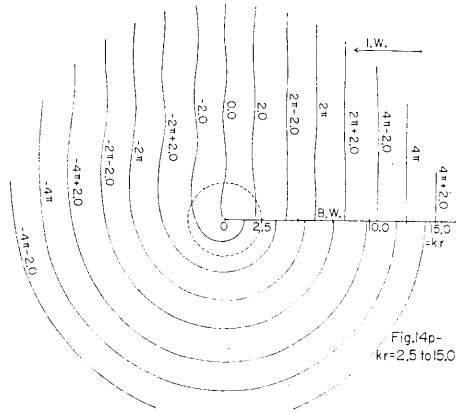

Figs. 10*p*–14*p*. Variation of the phase around the terminus of the single breakwater wing for lateral incidence (based on Stoker's theory). **I. W.** and **B. W.** stated in the figures are the abbreviation of "incident wave" and "breakwater".

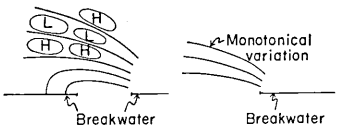

Fig. 15. Difference of the variation of the amplitude in two cases of the double and single breakwater wings. **H** and **L** are the abbreviations of high and low amplitudes.

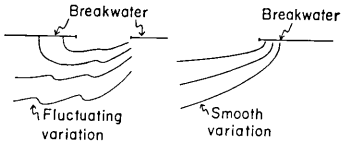

Fig. 16. Difference of the amplitude variation in the cases of the double and single breakwater wings.

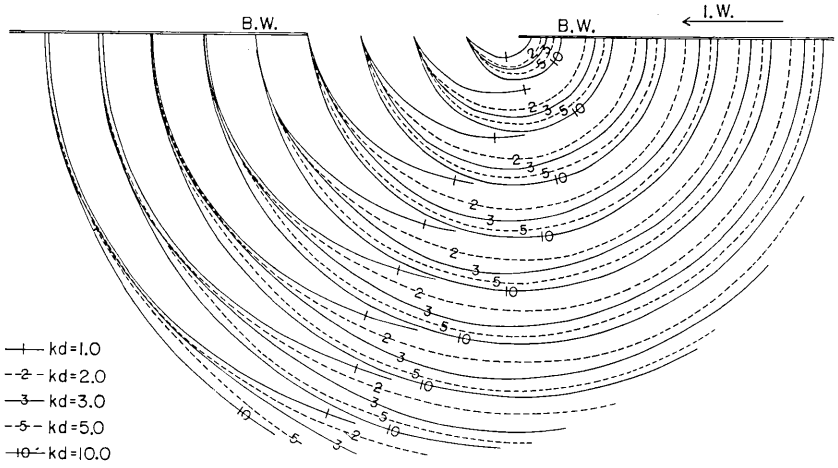

Fig. 17. Variation of the crest line in the leeward waters for change of kd.

facts are found. The contours of the phase in the range $kd=1.0$ to 10.0 are depicted in the same figure, *i.e.*, Fig. 17, to help the inspection of the variation of the crest line for the change of the wave-length. Fig. 17 shows that, when kd is small, the retardation of the wave behind the windward breakwater is large. As kd increases, the retardation begins to be small until the form of the crest line tends to a certain one which is probably shaped by Stoker's solution (*Stoker*, 1957) for the single breakwater with lateral incidence of the invading wave (see Fig. 18).

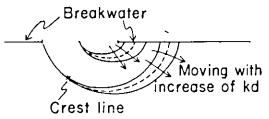

Fig. 18. Variation of the shape of the crest line in the leeward waters for the change of kd. The arrows stand for the moving sense of the shape of the crest line.

In Figs. 19$a(p)$ to 21$a(p)$, our results of the amplitude and phase variations (the case of the *double* breakwater wings) are compared with Stoker's (the case of the *single* breakwater wing with lateral incidence) to examine the validity of our theory and the extent of the effect of the leeward breakwater upon

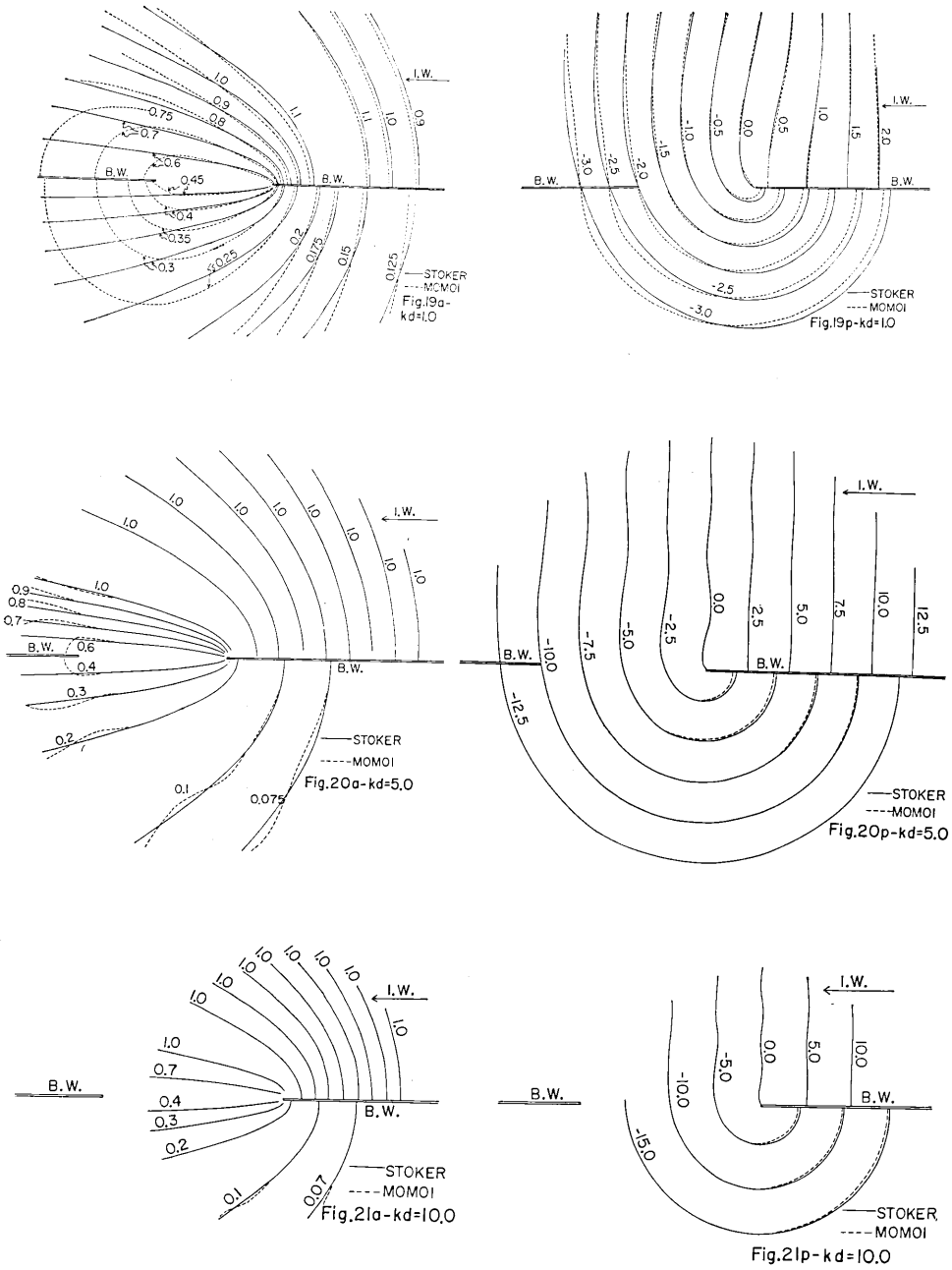

Figs. 19*a*(*p*)-21*a*(*p*). Comparison of the variations of the amplitude (phase) based on Momoi's and Stoker's theories, the former of which is the theory for the model of the double breakwater wings and the latter that for the single breakwater. The suffixes *a* and *p* denote the figures relevant to amplitude and phase. **I. W.** and **B. W.** stated in the figures are the abbreviation of "incident wave" and "breakwater".

the invading waves.** Figs. 19a and 19p (the figures for $kd=1.0$) reveal that the deviation of two authors' results is comparatively large in the nearby waters of the terminus of the leeward breakwater to suggest a large influence of the leeward breakwater upon the invading wave with long wave-length. The above deviation continues diminishing with the decrease of the wave-length (see Figs. 20$a(p)$ and 21$a(p)$ for $kd=5.0$ and 10.0), showing the diminishing effect of the leeward breakwater. Figs. 20$a(p)$ and 21$a(p)$ suggest that our method (the method of the buffer domain (*Momoi*, 1968b)) is well applicable to the present problems.

3. Reflection from the Leeward Breakwater

In this section, the effect of the leeward breakwater upon the invading wave is discussed. The discussing method is as follows.

Let $\bar{\zeta}_{double}$ be the conjugate value of the wave height ζ_{double} calculated by the procedure described in the fourth paper (*Momoi*, 1968b). The conjugate value of ζ_{double} denotes the wave height for the incident wave $\exp(iwt+ikx)$ instead of $\exp(-iwt-ikx)$. The subtraction of ζ_{single} $(\alpha=0)$ described in (1) from the above $\bar{\zeta}_{double}$ denotes *primarily* the reflection of the wave arrived at the leeward breakwater and the secondary reflection of the reflected wave from the leeward breakwater at the windward one. Let ζ_{ref} be a group of the reflected waves mentioned above, *i.e.*,

$$\zeta_{ref} \doteqdot \bar{\zeta}_{double} - \zeta_{single}(\alpha=0) \ , \qquad (2)$$

(refer to Fig. 22).

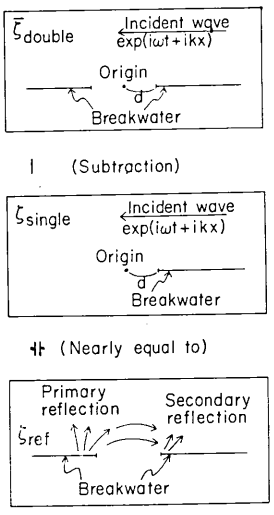

Fig. 22. Schema of equation (2).

In using expression (1), the origin of the coordinate is transferred to the point $(-d, 0)$ in the cartesian coordinate of Fig. 9. Expression (1) is then reduced to:

$$\zeta_{single}(\alpha=0) = e^{ikd}\left\{\frac{1}{2}J_0(kr_s) + \sum_{n=1}^{\infty} e^{i(n\pi/4)}J_{n/2}(kr_s)\cos\frac{n\theta_s}{2}\right\} , \qquad (3)$$

where

$$r_s = \sqrt{r^2-2rd\cos\theta+d^2} \ ,$$

$$\theta_s = \tan^{-1}(y_s/x_s) \ ,$$

** In using Stoker's solution, the origin is transferred to the midpoint of the breakwater gap. The expression is given in (3) of the following section.

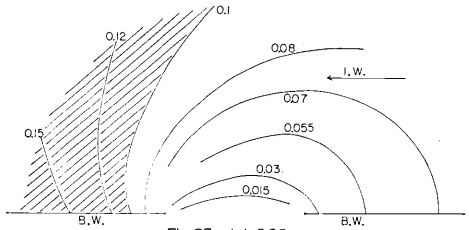

Fig.23a-kd=0.02

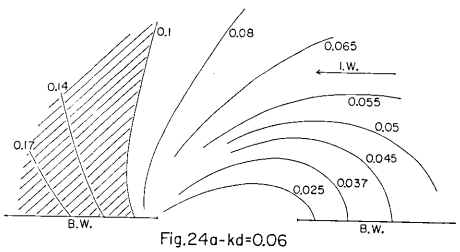

Fig.24a-kd=0.06

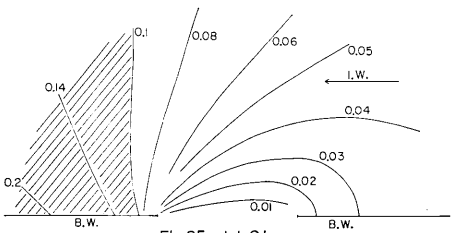

Fig.25a-kd=0.1

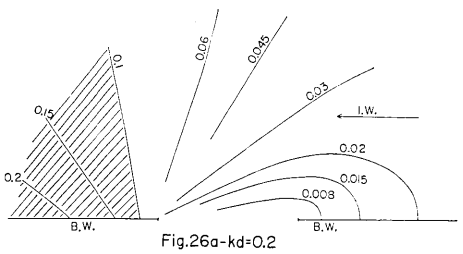

Fig.26a-kd=0.2

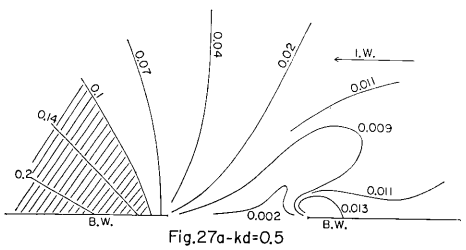

Fig.27a-kd=0.5

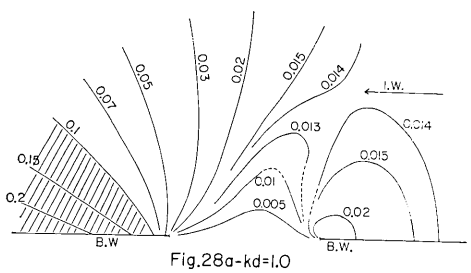

Fig.28a-kd=1.0

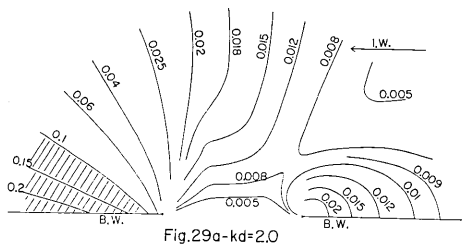

Fig.29a-kd=2.0

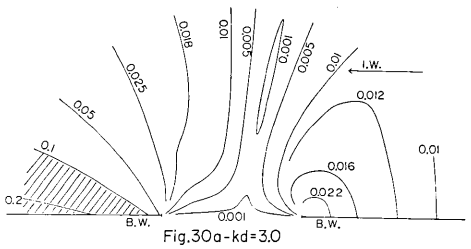

Fig.30a-kd=3.0

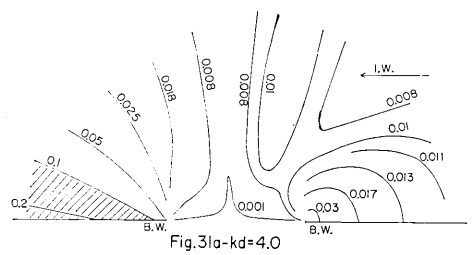

Fig.31a-kd=4.0

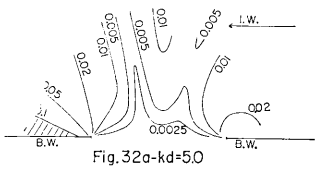

Fig.32a-kd=5.0

Figs. 23*a*–32*a*. Variation of the amplitude of the wave reflected from the leeward breakwater. **I. W.** and **B. W.** denote respectively "incident wave" and "breakwater.

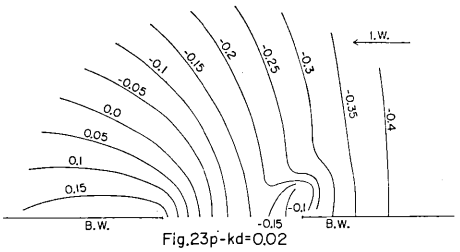

Fig.23p-kd=0.02

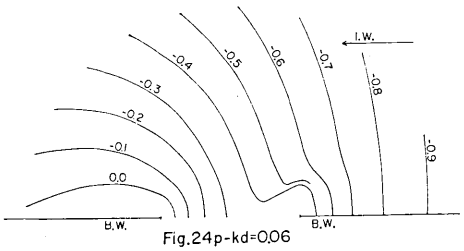

Fig.24p-kd=0.06

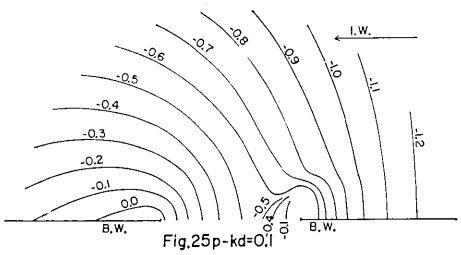

Fig.25p-kd=0.1

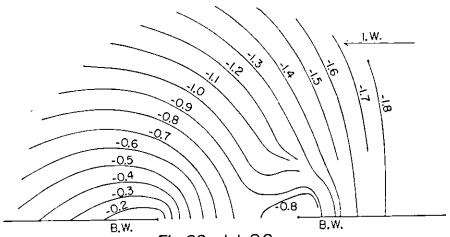

Fig.26p-kd=0.2

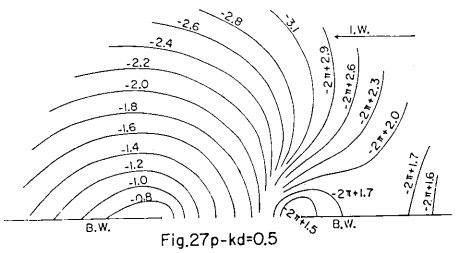

Fig.27p-kd=0.5

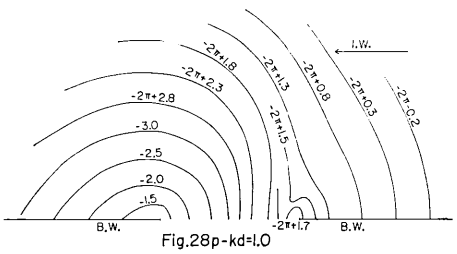

Fig.28p-kd=1.0

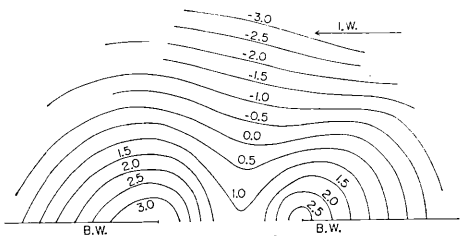

Fig.29p-kd=2.0

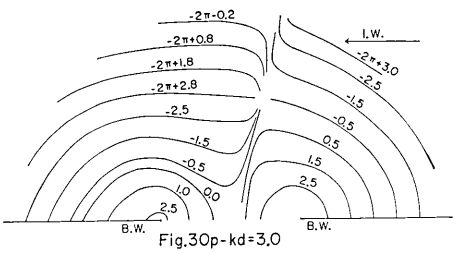

Fig.30p-kd=3.0

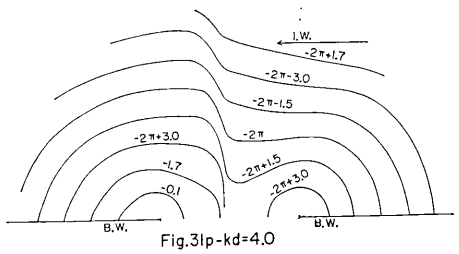

Fig.31p-kd=4.0

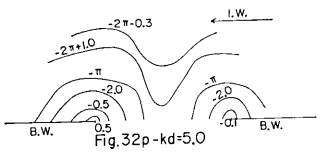

Fig.32p-kd=5.0

Figs. 23*p*-32*p*. Variation of the phase of the wave reflected from the leeward breakwater. **I. W.** and **B. W.** denote respectively "incident wave" and "breakwater".

$$x_s = r\cos\theta - d\ ,$$

$$y_s = r\sin\theta\ .$$

Using equation (2), the calculation of ζ_{ref} is made in the windward waters. The results are given in Figs. 23*a*(*p*) to 32*a*(*p*), in which the stated values are $|\zeta_{ref}|$ in Figs. 23*a* to 32*a* and arg ζ_{ref} in Figs. 23*p* to 32*p*.

In the figures concerning the variation of the amplitude (Figs. 23*a* to 32*a*), the region beyond $|\zeta_{ref}|=0.1$ is shaded, in which the reflected wave from the leeward breakwater is beyond 10 per cent of the incident wave in amplitude. The shaded region extends to the frontal area of the leeward breakwater for large wave-length, *i.e.*, $kd=0.02$ to 0.2 (Figs. 23*a* to 26*a*) with a disappearing tendency for the augmentation of kd (Figs. 27*a* to 32*a*). The above fact suggests a strong reflection of the invading wave from the leeward breakwater for small kd. Another high amplitude region appears in front of the *windward* breakwater, suggesting the secondary reflection (at the windward breakwater) of the wave reflected from the leeward breakwater (see Fig. 33).

As for the variation of the phase (Figs. 23*p* to 32*p*), the most conspicuous feature is the emitting wave from the leeward breakwater, which arrives at the windward breakwater to cause the kinking crest lines showing definitely the secondary effect of the windward breakwater upon the wave.

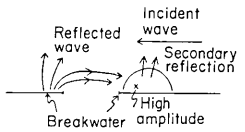

Fig. 33. Secondary reflection of the reflected wave at the windward breakwater.

References

Momoi, T., 1967a, A Long Wave around a Breakwater [I], *Bull. Earthq. Res. Inst.*, **45**, 91-136.

Momoi, T., 1967b, A Long Wave around a Breakwater [II], *Bull. Earthq. Res. Inst.*, **45**, 749-783.

Momoi, T., 1968a, A Long Wave around a Breakwater [III], *Bull. Earthq. Res. Inst.*, **46**, 125-135.

Momoi, T., 1968b, A Long Wave around a Breakwater [IV], *Bull. Earthq. Res. Inst.*, **46**, 319-343.

Momoi, T., 1968c, A Long Wave around a Breakwater [V], *Bull. Earthq. Res. Inst.*, **46**, 889-899.

Stoker, J.J., 1957, Water Waves, *Pure and applied mathematics, Vol. IV, Interscience Publishers, Inc., New York*, 109-147.

11. 防波堤のまわりにおける長波 [VI]
—— 横入射の場合 ——

地震研究所　桃　井　高　夫

本報告においては防波堤の近傍における長波（横入射の場合）が数値計算を通して論じられている．計算は防波堤が間隙をもつ（二の防波堤の）場合における合成波（*resultant wave*），および風下側の防波堤よりの反射波，更に単一防波堤の場合における合成波に対してなされている．最も著しい現象はこの防波堤の場合，風下側の防波堤よりの反射波の発生である．